Citation: BoneKEy Reports **4**, Article number: 654 (2015) | doi:10.1038/bonekey.2015.21

www.nature.com/bonekey

ORIGINAL ARTICLE

Missense mutation in the PTEN promoter of a patient with hemifacial hyperplasia

Kiyomi Yamazaki[1,2], Charis Eng[3,5], Sergei A Kuznetsov[4], John Reinisch[1], Dennis-Duke Yamashita[1], John Walker[1], Craig Cheung[2], Pamela G Robey[4] and Stephen L-K Yen[1,2,4]

[1]Childrens Hospital Los Angeles, Los Angeles, CA, USA. [2]Center for Craniofacial Molecular Biology, University of Southern California, Los Angeles, CA, USA. [3]Clinical Cancer Genetics Program, Human Cancer Genetics Program, Comprehensive Cancer Center, Department of Internal Medicine, The Ohio State University, Columbus, OH, USA. [4]Craniofacial and Skeletal Diseases Branch, National Institute of Dental and Craniofacial Research, National Institutes of Health, Bethesda, MD, USA.

The cellular mechanisms involved in the asymmetric facial overgrowth syndrome, hemifacial hyperplasia (HFH), are not well understood. This study was conducted to compare primary cell cultures from hyperplastic and normal HFH bone for cellular and molecular differences. Primary cultures developed from biopsies of a patient with isolated HFH showed a twofold difference in cell size and cell number between hyperplastic and normal bone. Microarray data suggested a 40% suppression of PTEN (phosphatase-tensin homolog) transcripts. Sequencing of the *PTEN* gene and promoter identified novel C/G missense mutation (position −1053) in the regulatory region of the PTEN promoter. Western blots of downstream pathway components showed an increase in PKBa/Akt1 phosphorylation and TOR (target of rapamcyin) signal. Sirolimus, an inhibitor of TOR, when added to overgrowth cells reversed the cell size, cell number and total protein differences between hyperplastic and normal cells. In cases of facial overgrowth, which involve PTEN/Akt/TOR dysregulation, sirolimus could be used for limiting cell overgrowth.

BoneKEy Reports **4**, Article number: 654 (2015) | doi:10.1038/bonekey.2015.21

Introduction

Isolated hemifacial hyperplasia (HFH) is[1–14] a rare condition of asymmetric facial growth occurring in 1/14 000–1/86 000 live births. It is also known as hemihypertrophy[15] and is sometimes associated with the Beckwith–Wiedemann syndrome, neurofibromatosis, the Proteus syndrome, the Klipper–Trenaunay–Weber syndrome and tumors of the liver, adrenal gland or kidney. The molecular etiology for HFH is not known (AHC (MIM: 235000)). Current treatments are based on surgically reducing the facial asymmetry and overgrown tissues, which can include the frontal bone, maxilla, palate, mandible, alveolar process, tongue, and teeth and associated soft tissues.[15,16]

As the facial features of HFH are similar to a group of facial hamartoma-like syndromes associated with an epidermal nevus (**Figure 1**),[17,18] one approach to understanding these disorder tests whether mutations in the tumor suppressor gene *PTEN* (phosphatase-tensin homolog) may be common to all syndromes of hamartomatous overgrowth.[19] Germline PTEN mutations have been reported in 85% of the Cowden syndrome, 65% of the Bannayan–Riley–Ruvalcaba syndrome,[20] 20% of the Proteus syndrome and 50% of the Proteus-like syndromes.[20,21] PTEN is an important regulator of cell growth via the insulin/insulin growth factor-I (IGF-I) and -II pathway as it can suppress cell growth via the PI3K/Akt pathway by decreasing phosphatidylinositol-3,4,5 triphosphate levels, which results in decreased Akt phosphorylation.[22] PTEN can also cause G_1 cell arrest and apoptosis in many cell types.[23,24] When PTEN is mutated or suppressed, Akt is inappropriately activated and signals the cell proliferation noted in many types of tumors.

A downstream component of the PI3K/Akt pathway is TOR (target of rapamcyin), which is a determinant of cell size in *Caenorhabditiselegans*, *Drosophila* and mouse models.[25–27] This study was conducted to develop a cell culture model for HFH by developing primary cultures from bone biopsies. Significant cell growth differences were retained in primary cultures derived from normal and overgrowth bone biopsies, as were alterations in PTEN, Akt and TOR signaling. In addition, the cell overgrowth, cell proliferation and increased protein content observed on the overgrown side were rescued by adding Sirolimus (rapamycin) to inhibit TOR.

Correspondence: Dr SL-K Yen, Center for Craniofacial Molecular Biology, CSA 103, 2250 Alcazar Street, Los Angeles, CA 90033, USA.
E-mail: syen@usc.edu
[5]Current address: Genomic Medicine Institute, Lerner Research Institute, Cleveland Clinic, OH, USA.

Received 13 September 2014; accepted 18 December 2014; published online 29 July 2015

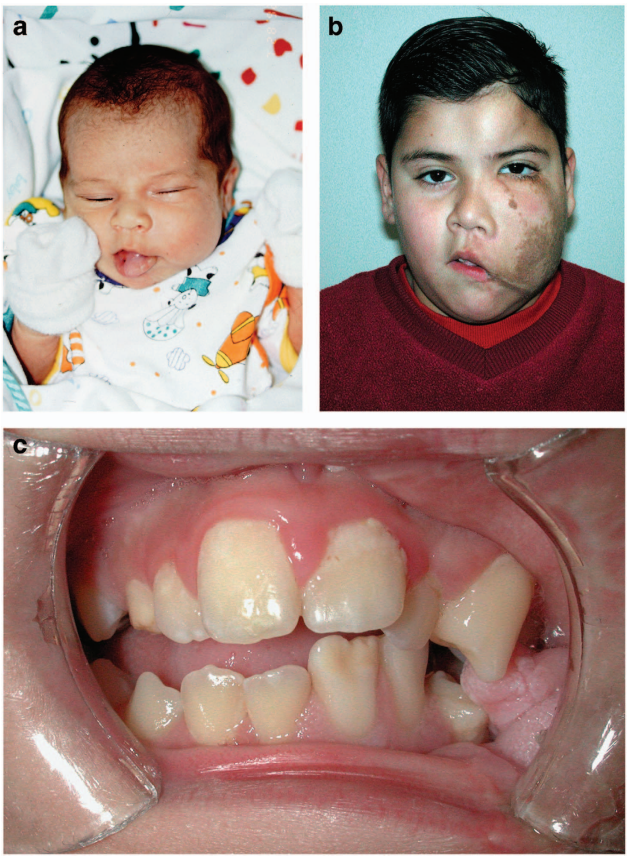

Figure 1 Hemifacial hyperplasia. Photographs showing the progressive nature of asymmetric enlargement: (**a**) birth; (**b**) 13 years and (**c**) enlargement of teeth and hyperplastic oral mucosa.

Results

Histopathology

Biopsies of the epidermal nevus showed characteristic parakeratotic areas, acanthosis and papillomatosis. Subcutaneous biopsies showed bundles of muscle separated by enlarged areas of adipose and fibrous tissue. In all specimens, there was an increase in vascularity ranging from sinusoidal vessels to large arteries and veins. Cheek specimens exhibited dense fibrous lipomatous tissue with mixed portions of salivary gland and striated muscle tissue. No lymphatic involvement was observed. Nerve hypertrophy was noted in all biopsied tissues. The most prominent feature in all of the skin specimens from the overgrowth side was an overabundance of nerves not observed in tissues from the normal side (**Figure 2**). Nerves under the skin, but not under the nevus, had a distinctive neuromatous appearance with lipocyte infiltration, abnormally thickened nerve trunks and increased number of nerves per unit area. Immunocytochemistry with the S100 antibody showed a high concentration of Schwann cells in the affected dermis (**Figures 2a–d**). Hyperplastic bone had a wide cortical plate and an increased number of osteocytes (**Figures 2d–f**).

Cell size and number differences

Primary cell cultures from the hyperplastic side(O) and normal side HFH bones were morphologically indistinguishable (**Figures 3a–d**). Hyperplastic and normal cells (**Figures 2c and d**) showed a maximal difference at 70% confluence during the first five passages: a 2.1-fold increase in size for HFH cells and a 2.4-fold increase in cell number. At 90% confluence, the difference was less: a 1.3-fold increase in size and 1.4-fold increase in HFH cell number. Cells at 70% confluence during the third passage were used for comparisons of gene expression. Both hyperplastic and normal HFH cells formed bone upon subcutaneous transplantation into immunocompromised mice.

Microarray analysis

When the Affymetrix Human HG-U95 Av.2 microarrays were compared using a twofold screen, 70 genes differed; a 1.5-fold screen produced 254 hyperplastic genes that either increased or decreased compared with the normal side cells. The top functions were related to cancer and cell proliferation of mesenchymal cells. The Ingenuity Pathway Analysis identified the IGF-I and glucocorticoid receptor as key pathways. In addition, 20 cell cycle regulator proteins were identified in the 1.5-fold screen that predicted a decrease in G2/M transition. There was a 40% relative reduction in PTEN expression in cells from hyperplastic side compared with the normal side.

PTEN expression and P13K/Akt1 pathway activation

Real-time RT-PCR confirmed the reduction of PTEN mRNA in overgrown cells relative to normal-side cells after normalization against β-actin control samples. Immunoprecipitation of Akt phosphorylation product showed a clear increase in Akt/PK phosphorylation in the hyperplastic HFH cells (**Figure 3f**). Western blot analysis detected more TOR protein and phosphorylated ribosomal S6 kinase in hyperplastic HFH cells compared with normal HFH cells (**Figures 3g and h**).

Genetic testing and PTEN mutational analysis

Cytogenetic analysis revealed no chromosomal abnormalities for this patient. There were also no deletions or missense mutations in the PTEN exons; however, a novel C/G germline missense mutation was detected in the promoter at position −1059 relative to the translational start site. This mutation lies between the Erg-1 (949–937) and p53 (−1190 to 1157) binding sites in the promoter region (**Figure 4**).

Sirolimus treatment of cells in primary culture

When cells from the overgrown side were exposed for 72 h to sirolimus at 50 ng ml^{-1}, the cells reverted to normal size, cell proliferation and protein content. Sirolimus compensated for the difference between overgrown and normal side by reducing the cell number of hyperplastic cells in primary cultures by 35.5%, by decreasing the protein content by 25.3% (**Figure 4b**) and by shifting the cell size toward a smaller cell size (**Figure 4c**).

Materials and Methods

This study was performed at the request of the patient's parents to better understand the etiology of HFH.

Patient diagnosis and history

This patient presented at Childrens Hospital Los Angeles as a newborn with a 'left swollen cheek'. With growth, his left forehead and malar region of the face became asymmetric and enlarged despite three surgical debulking procedures

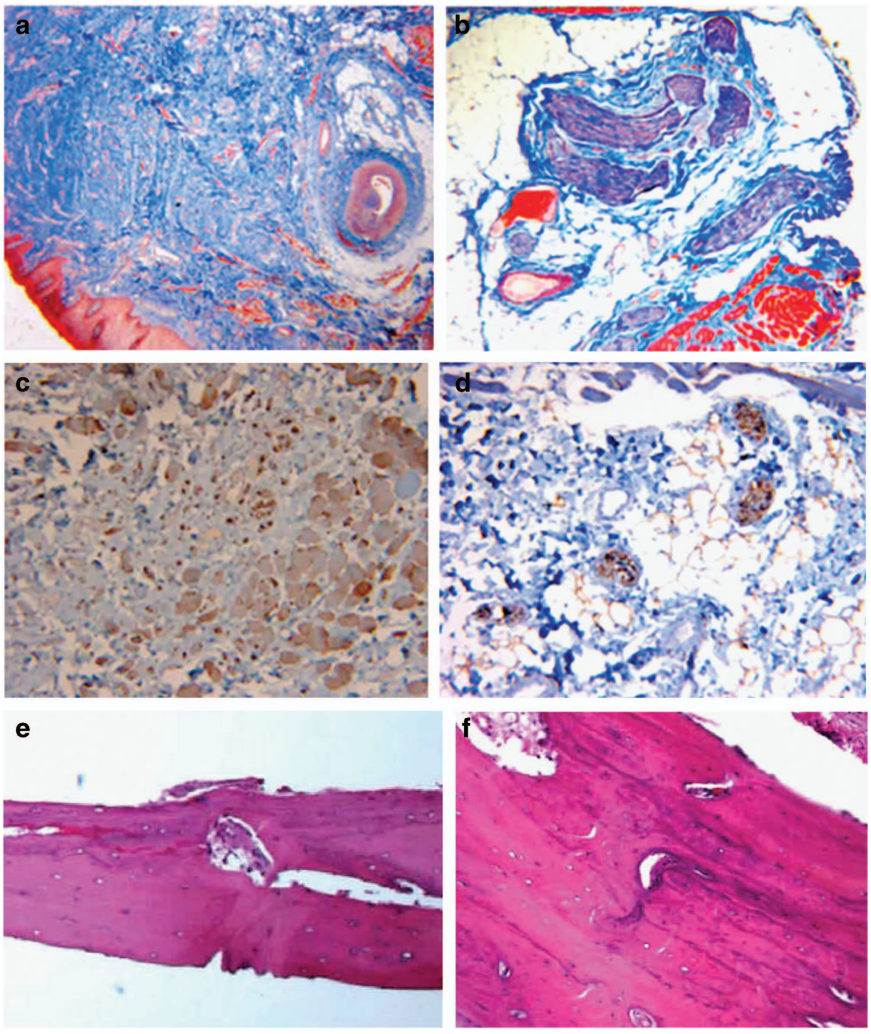

Figure 2 Histopathology. (**a** and **b**) Masson-Trichrome stained × 10 and × 40 photomicrographs of the dermis showing abnormally thickened nerve trunks. (**c** and **d**) S100 antibody stained × 10 and × 100 photomicrographs showing abnormal Schwann cells surrounding peripheral nerve axons and increased number of nerves per unit area, 'neuromatous appearance'. (**e**) Hemotoxylin- and eosin-stained photomicrographs of unaffected bone. (**f**) Affected bone showing increased width of cortical bone and increased number of osteocytes.

(**Figure 1**). There was no family history of facial overgrowth or hamartoma. He had a negative abdominal ultrasound and did not have additional orthopedic anomalies. At age 7 years, he had asymmetric hyperplasia of the tongue, tonsil, dentition, gingiva and cheek mucosa, as well as a distinct linear nevus covering the left cheek that extended to the postauricular region, dental crossbites, a left-sided tongue thrust and inferiorly displaced oral commissure, left eye presbyopia, left chronic otitis media and decreased motion of the left side of the face with animation. Two features not common to HFH were the epidermal nevus and left-sidedness of the anomaly. This patient lacked malformations of the extremities and cerebriform folds of the skin that are associated with the Proteus syndrome.[28,29] On radiographs, the skeletal borders of the growing bone were more consistent with expansive hyperplasia rather than ragged infiltrative lesions associated with the Proteus syndrome. Based on these features, the patient's condition was diagnosed as HFH rather than the Proteus syndrome.

Derivation of bone marrow stromal cells from surgical specimens

Patient consent for the use of tissue samples was obtained by Institutional Review Board-approved protocols. During surgical debulking, 3–18 mm of bone was removed from contralateral zygomatic regions of the maxilla and immediately placed in sterile growth medium. Bone marrow stromal cells were isolated and propagated *in vitro* according to a previously published technique.[30] Briefly, bone marrow was scraped from trabecular bone, pipetted to break up cell aggregates and filtered through a 70 μm nylon strainer (Bectin Dickinson, Franklin Lakes, NJ, USA) before culturing. A single-cell suspension of bone marrow cells was cultured in a growth medium consisting of α-MEM (α-minimum essential medium; Invitrogen, Grand Island, NY, USA), 2 mM L-glutamine, 100 U ml^{-1} penicillin, 100 μg ml^{-1} streptomycin sulfate (Biofluids, Rockville, MD, USA) and 20% fetal bovine serum of a preselected lot (Equitech-Bio, Kerrville, TX, USA). The cells were incubated at 37 °C in 100% humidity and 5% CO_2. Cell cultures derived from

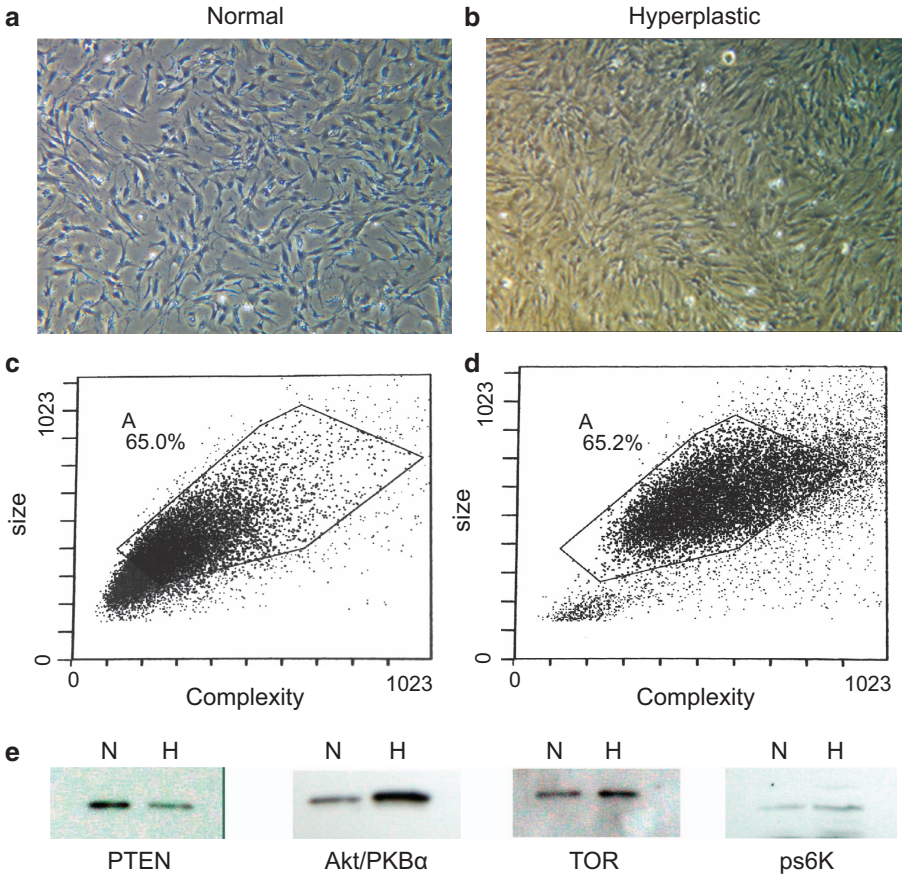

Figure 3 Cell culture model of hemifacial hyperplasia. Photomicrographs and flow cytometry of cell cultures seeded at the same initial cell concentrations: (**a**) normal HFH cells (N) after 2 days of growth; (**b**) hyperplastic (H) HFH cells after 2 days of growth; (**c**) size distribution of normal HFH cells at 70% confluence; (**d**) size distribution of overgrowth HFH cells at 70% confluence; (**e**) western blots and the Akt/phosphorylation assay showing anti-PTEN (1:100), Akt PKB phosphorylation, TOR and pS6K.

the overgrowth side were labeled 'hyperplastic HFH'. Cells derived from the unaffected side of the head were labeled 'normal HFH'. Third passage cells were used for *in vivo* transplantation assays to analyze their osteogenic potential[30] and for cell growth and gene expression assays. Frozen cell stocks were stored in 44% α-MEM, 50% fetal bovine serum, 1% penicillin/streptomycin and 5% dimethylsulfoxide (Sigma, St Louis, MO, USA) and carefully thawed for further analysis. Osteogenic potential was assayed by *in vivo* transplantation of single colonies into immunocompromised mice.[30,31]

Flow cytometry

To measure cell size, hyperplastic and normal HFH cell cultures were seeded at the same concentration and compared by flow cytometry when the cells reached 50%, 70% and 90% confluence based on manual cell counts. Trypsinized cells (10^6) were collected and scanned for relative cell size measurement in a flow set for forward light scatter and size scatter at the Flow Cytometry Core Facility, Institute of Genetic Medicine, USC.

Chromosome analysis

High-resolution chromosome studies were performed on HFH cell cultures at the Children's Hospital Los Angeles Cytogenetics Laboratory.

PTEN gene sequencing

PCR-based denaturing gradient gel electrophoresis and direct DNA sequencing of all nine PTEN exons and flanking intronic regions, deletion analysis of the *PTEN* gene and promoter sequencing were performed according to Zhou *et al.*[21] The full 600 bp PTEN promoter was sequenced from positions −1344 to −745 relative to the translational start site. A missense mutation with a C to G base substitution was identified at position −1058.

Microarray

RNA was column-purified, quantitated and reverse transcribed for microarray hybridization and analysis using Affymetrix Human HG-U95 Av.2 microarrays. RNA integrity was tested by 3′ to 5′ probe signal ratio of *β-actin* and *GAPDH* genes. Three microarray comparisons were performed between hyperplastic and normal HFH cell cultures grown to 70% confluence and analyzed using Ingenuity Pathway Analysis softwares (Redwood City, CA, USA).

Real-time PCR

Using the SYBR green protocol (iCycler; Bio-Rad Laboratories, Hercules, CA, USA), real-time PCR comparisons of hyperplastic and normal HFH cell RNA were conducted using dual temperature cycles of 60 °C and 94 °C with primers representing the PTEN (sense, 5′-TGTTGTTTCACAAGATGATGTTTGA-3′; antisense, 5′-CGTCGTGTGGGTCCTGAATT-3′) and β-actin

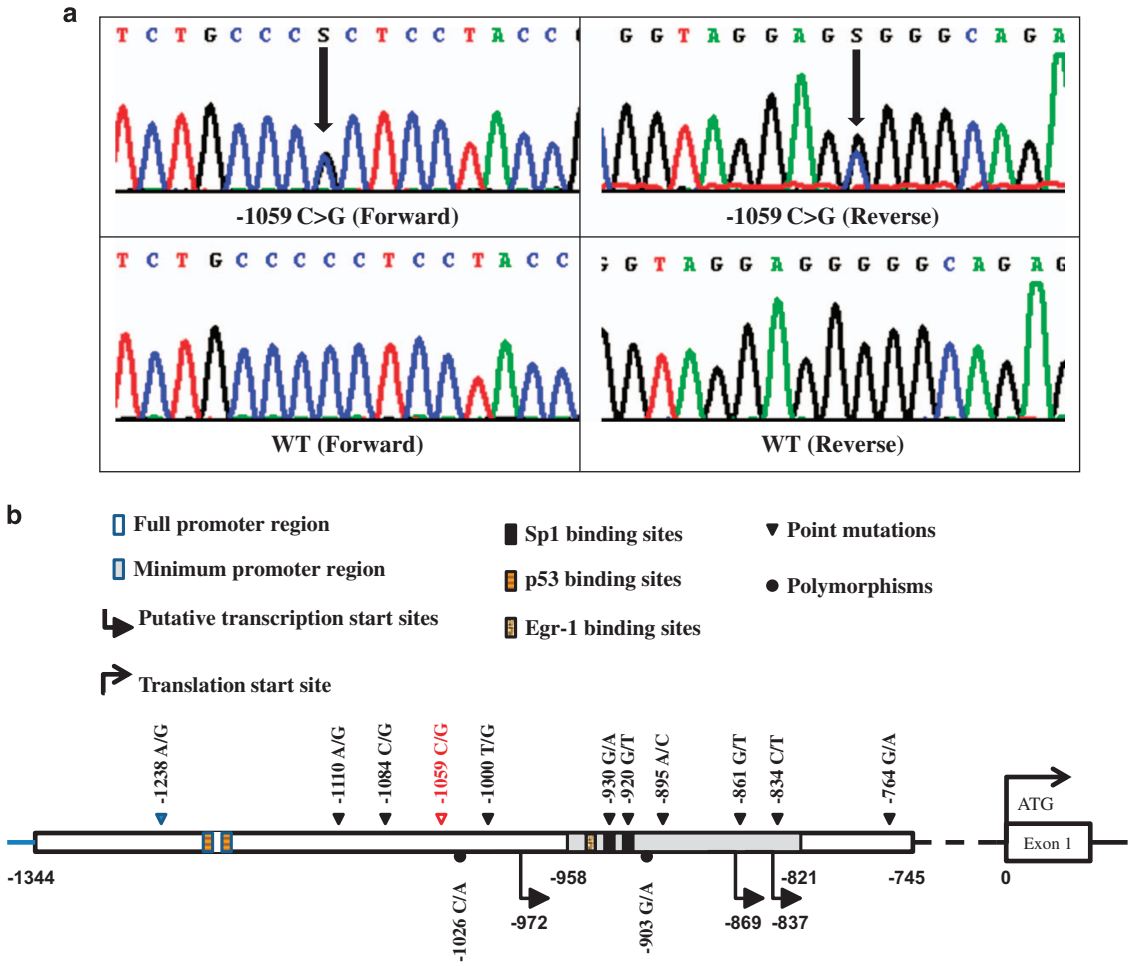

Figure 4 (**a**) Sequencing chromatogram of PTEN promoter showing mutation at − 1059 C > G single-nucleotide base pair change. (**b**) Schematic of PTEN promoter showing missense mutation is between Erg-1 and p53 binding sites.

(sense, 5′-GGGAAATCGTGCGTGACATC-3′; antisense, 5′-GCGGCAGTGGCCATCTC-3′) genes.

Western blot protein analysis

Whole-cell lysates from cell cultures were prepared by the boiling method, electrophoresed in 12% polyacrylamide gels (sodium dodecyl sulfate-polyacrylamide gel electrophoresis) and electroblotted onto polyvinylidene difluoride membranes, and then blocked for 1 h, exposed to primary antibodies at 100 μg per blot and secondary horseradish peroxidase-conjugated goat anti-rabbit IgG for 1 h at room temperature, reacted with substrate (Luminol/H_2O_2) according to the manufacturer's protocol (Roche, Indianapolis, IN, USA) and detected with Kodak X-Omat AR film (Kodak, Rochester, NY, USA). Primary antibodies directed against PTEN (Biocascade, Winchester, MA, USA), TOR (Cell Signaling, Woburn, MA, USA), phosphorylated ribosomal S6 kinase (pS6K), β-actin and GAPDH (the last three from Santa Cruz Biotechnologies, Santa Cruz, CA, USA) were used at 50–100 μg per blot. Protein content was analyzed by the Bradford assay (Bio-Rad Labs, Hercules, CA, USA).

Akt/PKBα kinase immunoprecipitation assay

A non-radioactive Akt/PKBα Kinase Immunoprecipitation Assay Kit (Upstate Cell Signaling Solutions, Lake Placid, NY, USA) was designed to measure phosphotransferase activity in an immunocomplex formed between the Akt/PKBα domain antibody and active Akt/PKBα. Immunoprecipitates were detected by an antiphospho-Akt antibody.

Sirolimus treatment of cell cultures

Overgrowth HFH and normal HFH cells were cultured at the same initial cell density (1×10^5 cells per ml) with 50 ng ml^{-1} sirolimus for 24, 48 and 72 h and harvested for manual cell count, flow cytometry analysis (1×10^6 cells) and for determination of protein content by the Bradford assay.

Discussion

The cell proliferation and overgrowth of cells isolated from bone biopsies corroborate a study by Yoshimoto *et al.*[32] on osteoblast cell cultures from HFH patients, which reported no morphological differences between hypertrophic and normal side cells but showed a threefold increase in cell proliferation on the overgrown side as measured by [^{3}H]thymidine incorporation. This patient shared many of the facial characteristics with Proteus syndrome such as a mosaic distribution of lesions, progressive course, sporadic occurrence, epidermal nevus, skull hyperostosis, vascular malformation, lipomatous

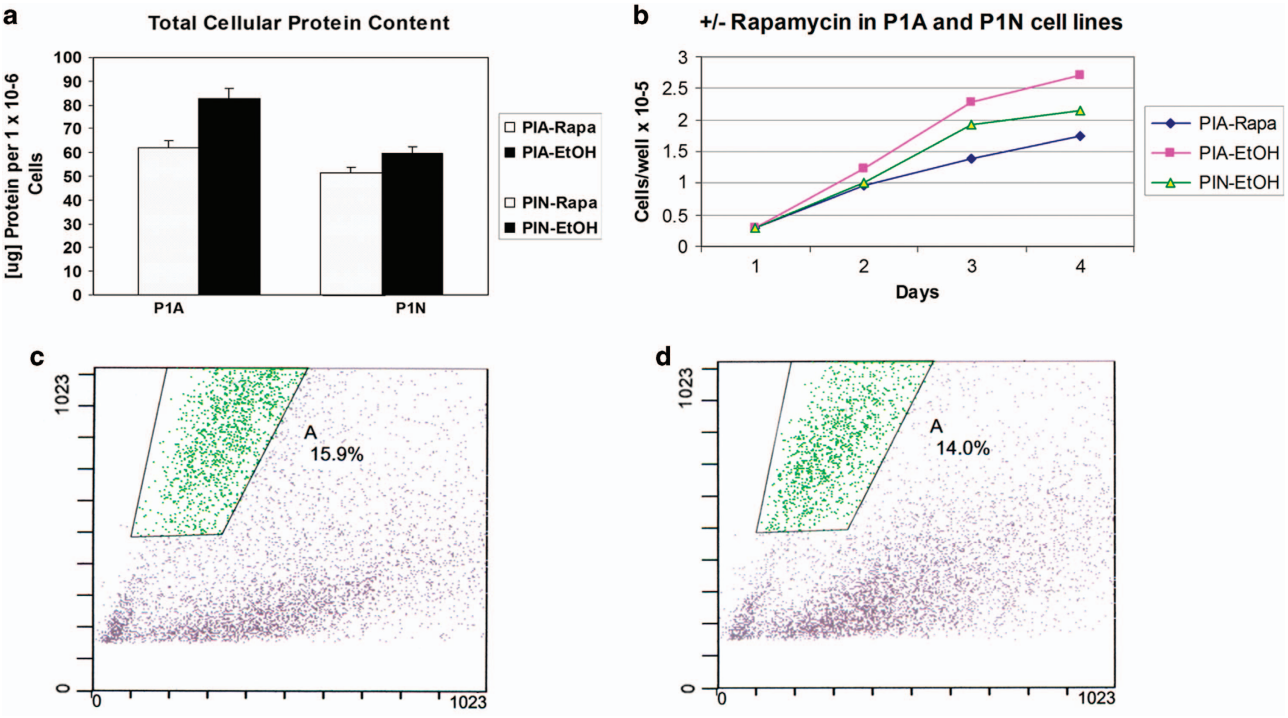

Figure 5 Sirolimus effects on the overgrowth HFH cell line. Overgrowth and normal HFH cells were initially plated at 1×10^5 cells per well and cultured in the absence or presence of 50 ng of sirolimus for 72 h. (**a**) Reduction in the number of sirolimus-treated overgrowth cells by 35.5% in comparison with non-treated overgrowth cells. (**b**) Decrease in total cellular protein content in overgrowth cells following sirolimus treatment for 72 h. (**c**) Untreated hyperplastic cells (**d**) shift in relative cell size with sirolimus treatment as measured by flow cytometry.

dysregulation and hemihyperplasia.[33] A novel finding was the histopathology, which also showed an unusually dense number of Schwann cells and blood vessels in the affected soft tissue biopsies and a large number of cells that were immunostained by the S100 antibody that was similar to a report by Gomez-Manzano *et al.*[34]

The *PTEN* gene and promoter were sequenced because germline *PTEN* mutations were found in 20% of patients with Proteus and Proteus-like syndromes.[20] This study identified a novel PTEN promoter mutation in a highly conserved region positioned between two putative transcription factor binding sites. This mutation is in the vicinity of at least three other Cowden-related germline promoter mutations that have been shown to affect PTEN protein and enhance Akt phosphorylation.[35]

Our experiments suggest that facial overgrowth may result from a downregulation of PTEN rather than a complete loss of PTEN function. With the discovery of germline *PTEN* mutations associated with hamartoma syndromes (**Figure 5**), Pilarski and Eng[36] proposed that a hamartoma-neoplasia syndrome with a germline *PTEN* mutation be classified as a *PTEN* hamartoma syndrome. Inoki *et al.*[18] proposed that dysregulation of mTOR is the common basis for hamartomas and for cellular hypertrophic disorders. A similar type of classification based on Akt1 has been proposed for the Proteus syndrome. Taken together, facial hamartomas can be grouped under PTEN/Akt1/TOR dysregulation overgrowth conditions.

In *Drosophila* and mice, TOR homologs Dros and mTor have been shown to regulate cell size.[37] As the TOR protein can be specifically inhibited by sirolimus, changes in TOR protein may lead to a method for suppressing the effects of upstream PTEN signals.

Although the cell culture model appears to replicate the *in vivo* cell growth and cell proliferation, the number of studies we were able to conduct was limited by our stock of primary cell cultures. Recurrent surgeries for debulking the asymmetry represent periodic opportunities to replenish stocks of HFH and normal cells during reconstructive surgery.

In conclusion, these experiments report a case of HFH with a missense mutation in the PTEN promoter and increased Akt phosphorylation. Primary cell cultures taken from the overgrowth side responded to sirolimus treatment by returning to a cell size and rate of proliferation comparable to the normal side. Animal studies are needed to determine whether HFH due to dysregulation of the PTEN/Akt. TOR pathway can be treated with sirolimus at the TOR branch point.

Conflict of Interest

The authors declare no conflict of interest.

Acknowledgements

This research was supported in part by the USC Center for Craniofacial Molecular Biology (MS and SL-KY), by the Marsh Robinson Society of Oral and Maxillofacial Surgeons (SL-KY), the American Cancer Society (RSG02-0151-01CCE to CE) and in part by the Division of Intramural Research, the National Institute of Dental and Craniofacial Research (SAK and PGR) (IRP, NIH, DHHS). CE is a recipient of the Doris Duke Distinguished Clinical Scientist Award. We appreciate the friendship of and suggestions from Drs Axel Schonthal and Deborah Johnson and the technical assistance of XP Zhou.

References

1. Scanga SE, Ruel K, Binari RC, Snow B, Stambolic V, Bouchard D *et al.* The conserved P13K/PTEN/Act signaling pathway controls both cell size and survival in *Drosophila. Oncogene* 2002; **19**: 3971–3977.
2. Kwon CH, Zhu X, Zhang J, Baker SJ. mTor is required for hypertrophy of Pten-deficient neuronal soma *in vivo*. *Proc Natl Acad Sci USA* 2003; **100**: 12923–12928.
3. Fingar DC, Salama S, Tsou C, Harlow E, Blenis J. Mammalian cell size is controlled by mTOR and it s downstream targets S6K1 and e1F4E. *Genes Dev* 2002; **16**: 1472–1487.
4. Alvarez B, Garrido E, Garcia-Sanz JA, Carrera AC. Phosphoinositide 3-kinase activation regulates cell division time by coordinated control of cell mass and cell cycle progression rate. *J Biol Chem* 2003; **278**: 26466–26473.
5. Becktor KB, Becktor JP, Karnes PS, Keller EE. Craniofacial and dental manifestations of Proteus syndrome: a case report. *Cleft Palate Craniofac J* 2002; **39**: 33–45Review.
6. Thierry V, Adamson ED, Baron V, Birle D, Mercola D, Mustelin T *et al.* The Egr-1 transcription factor directly regulates PTEN during irradiation-induced signaling. *Nat Cell Biol* 2001; **3**: 1124–1128.
7. Stambolic V, MacPherson D, Sas D, Lin Y, Snow B, Jang Y *et al.* Transcriptional regulation of PTEN by p53. *Mol Cell* 2001; **8**: 317–325.
8. Sheng XY, Koul D, Liu JL, Liu TJ, Yung WK. Promoter analysis of tumor suppressor gene PTEN: identification of minimum promoter region. *Biochem Biophys Res Commun* 2002; **292**: 422–426.
9. Kwon. CH, Zhu X, Zhang J, Baker SJ. mTor is required for hypertrophy of Pten-deficient neuronal soma *in vivo*. *Proc Natl Acad Sci USA* 2003; **100**: 12923–12928.
10. Fingar DC, Richardon CJ, Tee AR, Cheatham L, Tsou C, Blenis J. mTor controls cell cycle progression through its cell growth effectors s6K1 and 4 E-BP1/eucaryotic translation initiation factor 4E. *Mol Cell Biol* 2004; **24**: 200–216.
11. Edinger AL, Linardic CM, Chiang GG, Thompson CB, Abraham RT. Differential effects of rapamycin on mammalian target of rapamycin signaling functions in mammalian cells. *Cancer Res* 2003; **63**: 8451–8460.
12. Neshat MS, Mellinghoff IK, Tran C, Stiles B, Thomas G, Petersen R *et al.* Enhanced sensitivity of PTEN-deficient tumors to inhibition of FRAP/ mTOR. *Proc Natl Acad Sci USA* 2001; **98**: 10314–10318.
13. Eng C. Will the real Cowden syndrome please stand up: revised diagnostic criteria. *J Med Genet* 2000; **37**: 828–830.
14. Reik W, Brown KW, Slatter RE, Sartor P, Elliott M, Maher ER. Allelic methylation of H19 and IGF2 in the Beckwith–Wiedemann syndrome. *Hum Mol Genet* 1994; **3**: 1297–1301.
15. Cohen MM, Neri G, Weksberg R. *Overgrowth Syndromes* New York, NY, USA: Oxford University Press, 2002.
16. Biesecker LG, Happle R, Mulliken JB. Proteus syndrome: diagnostic criteria, differential diagnosis, and patient evaluation. *Am J Med Genet* 1999; **84**: 389–395review.
17. Chen Y-R, Bendor-Samuel RL, Huang C-S. Hemimandibular Hyperplasia. *Plast Reconstr Surg* 1996; **97**: 730–737.
18. Inoki K, Corradetti MN, Guan KL. Dysregulation of the TSC-mTOR pathway in human disease. *Nat Genet* 2005; **37**: 19–24.
19. Eng C. PTEN: one gene, many syndromes. *Hum Mutat* 2003; **22**: 183–198review.
20. Zhou XP, Hampel H, Thiele H, Gorlin RJ, Hennekam RC, Parisi M *et al.* Association of germline mutation in the PTEN tumour suppressor gene and Proteus and Proteus-like syndromes. *Lancet* 2001; **358**: 2079–2080.
21. Zhou XP, Marsh DJ, Hampel H, Mulliken JB, Gimm O, Eng C. Germline and germline mosaic PTEN mutations associated with a Proteus-like syndrome of hemiphypertrophy, lower limb asymmetry, arteriovenous malformations and lipomatosis. *Hum Mol Genet* 2001; **23**: 13043–13048.
22. Stambolic V, Suzuki A, de la Pompa JL, Brothers GM, Mirtsos C, Takehiko S *et al.* Negative regulation of PKB/Akt-dependent cell survival by the tumor suppressor PTEN. *Cell* 1998; **95**: 29–39.
23. Gorberdhan DCI, Wilson C. PTEN: tumor suppressor, growth multifunctional regulator and more. *Hum Mol Genet* 2003; **12**: 239–248.
24. Leslie NR, Downes CP. PTEN function: how normal cells control it and tumor cells lose it. *Biochem J* 2004; **382**: 1–11.
25. Edinger AL, Thompson CB. Akt maintains cell size and survival by increasing mTOR-dependent nutrient uptake. *Mol Biol Cell* 2002; **13**: 2276–2288.
26. Faridi J, Fawcett J, Wang L., Roth RA. Akt promotes increased mammalian cell size by stimulating protein synthesis and inhibiting protein degradation. *Am J Physiol Endocrinol Metab* 2003; **285**: E964–E972.
27. Zheng X, Stokoe D, Kane L, Weiss A. The inducible expression of the PTEN tumor suppressor gene promotes apoptosis and cell size decrease by inhibiting P13K/Akt pathway in Jurkat T cells. *Cell Growth Differ* 2002; **13**: 285–296.
28. Turner T, Cohen MM, Biesecker LG. Reassessment of the Proteus syndrome literature: application of diagnostic criteria to published cases. *Am J Med Genet* 2004; **130**: 111–122.
29. Cohen MM, Turner JT, Biesecker LG. Proteus syndrome: misdiagnosis with PTEN mutations. *Am J Med Genet* 2003; **122**: 323–324.
30. Kresbach PH, Kuznetsov SA, Satomura K, Emmons RVB, Rowe DW., Gehron Robey P. Bone formation *in vivo*: comparison of osteogenesis by transplanted mouse and human marrow stromal fibroblasts. *Transplantation* 1997; **63**: 1059–1069.
31. Kuznetsov SA, Kresbach PH, Satomura K, Kerr M, Riminucci J, Gehron Robey P *et al.* Single-colony derived strains of human marrow stromal fibroblasts form bone after transplantation *in vivo*. *J Bone Miner Res* 1997; **12**: 1335–1347.
32. Yoshimoto H, Yano H, Kobyash K, Hirano A, Motomura K, Ohtsuru A *et al.* Increased proliferative activity of osteoblasts in congenital hemifacial hypertrophy. *Plast Reconstr Surg* 1998; **102**: 1605–1610.
33. Clark RD, Donnai D, Rogers R, Cooper J, Baraitser M, Opitz JM *et al.* Proteus syndrome: an expanded phenotype. *Am J Med Genet* 1987; **27**: 99–117.
34. Gomez-Manzano C, Fueyo C, Jian H, Glass TL, Lee H-Y, Liu J-L *et al.* Mechanisms underlying PTEN regulation of vascular endothelial growth factor and angiogenesis. *Ann Neurol* 2002; **53**: 109–117.
35. Zhou XP, Waite KA, Pilarski R, Hampel H, Fernandez MJ, Bos C *et al.* Germline promoter mutations and deletions in Cowden/Bannayan–Riley–Ruvalcaba syndrome result in aberrant PTEN protein and dysregulation of phosphoinositol-3-kinase/Akt pathway. *Am J Hum Genet* 2003; **73**: 404–411.
36. Pilarski R, Eng C. Will the real Cowden syndrome please stand up(again)? Expanding mutational and clinical spectra of the PTEN hamartoma syndrome. *J Med Genet* 2004; **41**: 323–326.
37. Backman S, Stambolic V, Mak TW. PTEN function in mammalian cell size regulation. *Curr Opin Neurobiol* 2002; **12**: 516–522.